Published in final edited form as:
J Immunol. 2013 December 1; 191(11): . doi:10.4049/jimmunol.1301604.

Regulation of Apoptosis and Innate Immune Stimuli in Inflammation Induced Preterm labor

Mukesh K. Jaiswal[*,§], **Varkha Agrawal**[#,§], **Timothy Mallers**[*], **Alice Gilman-Sachs**[*], **Emmet Hirsch**[#,¶], and **Kenneth D. Beaman**[*]

[*]Department of Microbiology and Immunology, Rosalind Franklin University of Medicine and Science, North Chicago, IL, USA

[#]Department of Obstetrics and Gynecology, NorthShore University HealthSystem, Evanston, IL

[¶]Department of Obstetrics and Gynecology, Pritzker School of Medicine, University of Chicago, Chicago, IL

Abstract

An innate immune response is required for successful implantation and placentation. This is regulated in part by a2 isoform of V-ATPase (a2V) and the concurrent infiltration of M1 (inflammatory) and M2 (anti-inflammatory) macrophages to the uterus and placenta. The objective of present study was to identify the role of a2V during inflammation-induced preterm labor in mice and its relationship to the regulation of apoptosis and innate immune responses. Using a mouse model of infection-induced preterm delivery, gestational tissues were collected 8 hrs after intrauterine inoculation on day 14.5 of pregnancy with either saline or peptidoglycan (PGN, a toll-like receptor (TLR) 2 agonist) and polyinosinic:cytidylic acid (poly(I:C), a TLR3 agonist), modeling Gram positive bacterial and viral infections, respectively. Expression of a2V decreased significantly in the placenta, uterus, and fetal membranes during PGN+poly(I:C) induced preterm labor. Expression of iNOS was significantly upregulated in PGN+poly(I:C) treated placenta and uterus. PGN+poly(I:C) treatment disturbed adherens junction proteins and increased apoptotic cell death via extrinsic pathway of apoptosis among uterine decidual cells and spongiotrophoblast. F4/80+ macrophages were increased and polarization was skewed in PGN +poly(I:C) treated uterus toward double positive CD11c+ (M1) and CD206+ (M2) cells, which are critical for the clearance of dying cells and rapid resolution of inflammation. Expression of *Nlrp3* and activation of caspase-1 was increased in PGN+poly(I:C) treated uterus which could induce pyroptosis. These results suggest that double hit of PGN+poly(I:C) induces preterm labor via reduction of a2V expression and simultaneous activation of apoptosis and inflammatory processes.

Introduction

Preterm birth is considered to be the most important cause of neonatal morbidity and mortality not due to congenital anomalies in the developed world (1). Up to 40% cases of preterm births occurs in association with microbial invasion of the gestational compartment (2). Although in individual cases it may be difficult to determine whether infection is a cause or a consequence of labor, it has become clear that infection and inflammation represent important and frequent mechanisms of disease.

Correspondence: Dr. Kenneth D. Beaman, Microbiology and Immunology, Rosalind Franklin University of Medicine and Science, 3333 Green Bay Road, N. Chicago, IL 60064, USA. kenneth.beaman@rosalindfranklin.edu.
[§]Contributed equally to this work.

Toll like receptors (TLRs) are a family of membrane bound proteins that recognize pathogen-associated molecular patterns and mediate innate immune responses (3–6). Binding of TLRs is the initial event in activation of the innate immune system which leads, among other events, to the nuclear translocation of the transcription factor nuclear factor (NF)-κB and the elaboration of a network of inflammatory mediators. We have shown that preterm labor can be induced in mice by pathogen-derived TLR ligands for TLR2 (peptidoglycan (PGN), 22%), TLR3 (polyinosinic:cytidylic acid (poly(I:C)), 14%), and in a synergistic fashion, TLR2 plus TLR3 (100%) (7). Using this well-validated mouse model of infection-induced preterm delivery, we and others have demonstrated previously that combined activation of TLR2 and TLR3 using PGN and poly(I:C) yields a dramatic synergy in the labor response and expression of inflammatory mediators in gestational tissues (7–10). Such combined stimulation might occur in nature in at least four scenarios: 1) engagement of TLR4; 2) activation of both TLR3 and another TLR simultaneously by a single organism (e.g., murine cytomegalovirus, herpes simplex virus, and Schistosoma mansoni (11, 12)); 3) superinfection, in which a host is infected simultaneously by more than one microorganism, such as a virus and a bacterium (13); and 4) activation of TLRs by one of several known, endogenously produced TLR ligands together with an exogenous pathogen (14, 15).

a2V-ATPase is a protein that is expressed in many mammalian cells and is involved in immune regulation and apoptosis. a2V-ATPase is the a2 isoform of the ‘a’ subunit of vacuolar ATPase, the enzyme that is present in intracellular vesicles and in the plasma membrane of specialized cells (16). One main function of V-ATPases is the acidification of intracellular compartments, a process which is crucial for many cellular functions (16). The a2 isoform of V-ATPase (a2V) is required for normal implantation, placental development and spermatogenesis (17–19). Expression of V-ATPase subunits in the bovine endometrium is crucial for trophoblast invasion and cellular communication (20). Our previous studies have shown that for successful implantation and placentation, a definite innate immune response is generated, which is regulated in part by a2V with the concurrent infiltration of M1 (inflammatory) and M2 (anti-inflammatory) macrophages in the uterus and placenta (17, 18). We have also shown that during LPS-induced fetal resorption, the decrease of placental a2V expression was associated with upregulation of proinflammatory cytokines (17).

The internal acidification of intracellular compartments such as lysosomes, endosomes, the Golgi complex, and secretary granules, has been suggested to play an important role in the mechanism of cell survival. V-ATPase plays an important role in the regulation of activity in organelles of the central vacuolar system. The V-ATPase inhibitors such as concanamycin A (21) or bafilomycin A1 (22) induce apoptosis in various cells such as a pancreatic cancer cell line (23) and RAW 264.7 (mouse macrophage) cells (24). Specifically, our lab has also shown that anti-a2V antibody induces activation of caspase-3 and is associated with apoptosis in T-lymphocytes (25). Two major apoptotic pathways (intrinsic and extrinsic) are active in cellular apoptosis (26). The intrinsic pathway involves the release of cytochrome c from the mitochondria into the cytosol where it binds to apoptotic protease activating factor (Apaf)-1. This results in the activation of the caspase-9 as well as induction of proteolytic activity by the executioner caspases −3, −6, −7, and finally in cleavage of PARP (Poly (ADP-ribose) polymerase) (26–28). The extrinsic pathway for apoptosis involves death receptors such as Fas which binds to its ligand, Fas L. The binding of Fas L to Fas induces the recruitment of the Fas/FADD complex. This Fas/FADD complex recruits initiator caspase-8 or −10 which also can activate the effector caspases −3,−6, and −7 and cleavage of PARP (29, 30).

a2V regulates apoptosis and delicate cytokine and chemokine networks for successful implantation (18, 31), placental development and growth at the feto-maternal interface (17). We hypothesized that a2V is an important factor in the regulation of the immune response in

pregnancy and may be involved, in part, in infection-induced preterm labor. Here we examined the role of a2V in PGN+poly(I:C) induced preterm labor in the mouse model and characterized its association to apoptosis and innate immune responses. We find that PGN +poly(I:C) induces preterm labor via simultaneous activation of apoptosis and inflammatory processes, and that a2V might be a bridge between these two processes.

Materials and Methods

Mice

For pregnancy outcome experiments, CD-1 female mice in estrus were selected by the gross appearance of the vaginal epithelium and were impregnated naturally. Mating was confirmed by the presence of vaginal plug. Intrauterine (IU) injections were performed on day 14.5 of a 19–20 day gestation, as previously described (32). Briefly, animals were anesthetized with 0.015 ml/g body weight of Avertin (2.5% tribromoethyl alcohol and 2.5% tert-amyl alcohol in PBS). A 1.5 cm midline incision was made in the lower abdomen. In the mouse, the uterus is a bicornuate structure in which the fetuses are arranged in a 'beads-on-a-string' pattern. Mice underwent injection of either (a) PGN (0.3mg/mouse) plus poly(I:C) (1.0 mg/mouse), or (b) saline. PGN and poly(I:C) were combined because we showed previously that this results in synergistic effects (both preterm delivery and inflammatory responses), a phenomenon that is mediated by both the MyD88-dependent and the MyD88-independent signaling pathways downstream of the TLR receptors (7). Each of the above intrauterine injections was performed in the midsection of the right uterine horn at a site between two adjacent fetuses, taking care not to inject individual fetal sacs. This dose of PGN+poly(I:C) causes delivery within 12–18 hrs after injection (7). Delivery of one or more pups in the cage or lower vagina within 48 hours was considered preterm. This model been shown to reproduce faithfully many aspects of infection-induced preterm labor in women, including the expression of cytokines, prostaglandins and other mediators; the lack of dependence on a drop in circulating progesterone; neonatal brain injury; and other characteristics (32–34). Surgical procedures lasted approximately 10 minutes. The abdomen was closed in two layers, with 4-0 polyglactin sutures at the peritoneum and wound clips at the skin.

Tissue harvest

Animals were euthanized 8 hours after surgery in order to examine tissue-level phenomena in an intrapartum state. Mice injected with PGN+poly(I:C) deliver in 12–18 hrs. The inoculated horn was incised longitudinally along the anti-mesenteric border. Gestational tissues (uteri (full thickness biopsies from the middle region), fetal membranes (pooled from all conceptuses in the injected uterine horn), fetuses and placentas) were harvested, washed in ice-cold PBS and either flash-frozen in liquid nitrogen and stored at −85°C for later RNA or protein extraction or fixed in 10% neutral buffered formalin for immunohistochemistry.

Cell culture

RAW 264.7 cells were cultured in DMEM High Glucose (GIBCO 11965-092) supplemented with 10% fetal bovine serum, 1% streptomycin and 1% penicillin in tissue culture flasks at 37°C in 5% CO_2/95% air and were passaged every 2 or 3 days to maintain logarithmic growth. Prior to each experiment, cells (4×10^4 cells per well) were plated in triplicate in 24-well plates and cultured overnight.

Cells were initially incubated for 2 hours with either PBS or PGN plus poly(I:C) (1μg/ml plus 10μg/ml) and then sequentially incubated for 3 hrs with either ATP (1mM), IgG (3μg/ml), anti-a2V (3μg/ml) and ATP plus anti-a2V. Experiment was conducted in triplicate and repeated twice.

Real-time PCR

Total RNA from gestational tissues was extracted after homogenization in Trizol reagent (Invitrogen, Carlsbad, CA) according to the manufacturer's protocol. For the cells, at the end of cell culture experiments, medium was aspirated and cells were washed with PBS and lysed in the wells with TRIzol. Quantity and integrity of RNA were confirmed by the ratio at 260:280 nm and electrophoresis was performed on 1.5% native agarose gel to visualize 18S and 28S ribosomal RNA subunits. Samples were stored at −80°C until further use. Two μg of total RNA were used as a template for cDNA synthesis. cDNA was prepared using random primers and the Moloney Murine Leukemia Virus (MMLV) reverse transcriptase system (Invitrogen, Carlsbad, CA).

Duplex RT-PCR was performed with one primer pair amplifying the gene of interest and the other an internal reference (GAPDH) in the same tube using the Applied Biosystems Step One Real-time PCR system. The prevalidated Taqman gene expression assays for a2V (*Atp6v0a2*, Mm00441848_m1); trophoblast development markers, *Hox10* (Mm00432549_m1) and *Hbegf* (Mm00439306_m1); cytokines *Mcp1* (Mm00441242_m1), *Nos2* (Mm00440502_m1) and TNF Mm00443258; macrophage markers *F4/80* (*Emr1*, Mm00802529_m1), *CD11c* (Mm00498698_m1), *CD206* (Mm00485148_m1), *CD209a* (Mm00460067_m1) and *Arg1* (Mm00475988_m1); inflammasomes markers *Nlrp3* (Mm00840904_m1) and *caspase-1* (Mm00438023_m1) and internal control *Gapdh* (4352339E) were purchased from Applied Biosystems (Foster City, CA). Real-time PCR was performed using universal PCR master mix reagent (Applied Biosystems). Use of TaqMan PCR Reagent Kits was in accordance with the manufacturer's manual. Reactions were performed in a 10μL mixture containing 0.5μL cDNA. PCR assays were performed in duplicate for each of the tissue sample.

Antibodies

Primary antibodies were as follows: mouse anti-a2V, rabbit anti-a2NTD (Covance, Denver, PA); rabbit anti-GAPDH (Cell signaling, Danvers, MA); mouse anti-iNOS, rabbit anti-FAS, rabbit anti-FasL, rabbit anti-FADD, rabbit anti-Bax, mouse anti-Bcl2, rabbit anti-E-cadherin, rabbit anti-N-cadherin, rabbit anti-β-catenin, rabbit anti-active caspase-3 (recognizes the p17 fragment of the active caspase 3) and rabbit anti-caspase-1, rat anti-F4/80, mouse anti-ITGAX (CD11c), mouse anti-CD206 (Abcam, Cambridge, MA); mouse anti-cleaved caspase-8 (recognizes the cleaved fragment of caspase-8 resulting from cleavage at Asp384), rabbit anti-cleaved caspase-9 (recognizes the cleaved fragment of caspase-9 resulting from cleavage at Asp330), (Cell Signaling technology). Isotype control antibodies were as follow: rat IgG isotype, mouse IgG isotype and rabbit IgG isotype (Abcam). Secondary antibodies were as follows: goat anti-rabbit IgG-FITC, goat anti-rabbit IgG AF-594 (Invitrogen), rabbit anti-rat IgG-FITC (Abcam), goat anti-rabbit IgG-HRP (Santa Cruz Biotechnology, Santa Cruz, CA), donkey anti-rabbit IRDye-800CW (LI-core Bioscience, Lincoln, NE) and EnVision + dual link System-Horseradish peroxidase (HRP) (Dako, Carpinteria, CA).

Immunohistochemistry and Immunofluorescence

The placenta and uterine horns were collected from control and PGN+poly(I:C) treated groups. Tissues were fixed in 10% neutral-buffered formalin at 4°C overnight and rinsed in PBS and infused with 30% sucrose solution at 4°C overnight or until the tissue sank. The tissues were snap frozen in OCT (Tissue-Tek, CA) in liquid nitrogen. Frozen tissue was stored at −80°C until further use. 5-μm sections from frozen tissues were mounted onto saline-coated glass slides (Dako) and stored at −80°C until used. The Dako EnVision + dual link System-HRP (DAB+) (Dako) was used to stain the frozen sections according to the

manufacturer's instructions with slight modifications. The sections were heated in the microwave in sodium citrate buffer (pH=6) for antigen retrieval.

For the detection of a2V protein, sections were incubated with 20μg/ml of antibody in 1% BSA-PBS for one hour at room temperature. Other antibody concentrations were as follows: For the pro-apoptotic marker Bax, anti-apoptotic maker Bcl2, and cytokine iNOS: 2μg/ml; for gap-junction proteins E-cadherin and N-cadherin: 10μg/ml; for FAS, FasL, and FADD: a 1:1000 dilution; for active caspase-8 and −9: a 1:100 dilution of antibody overnight at 4°C. After washing, sections were incubated with secondary antibody EnVison+ dual link system-HRP labeled polymer anti-mouse and anti-rabbit IgG. The chromogen 3,3'diaminobenzidine was used as substrate for the EnVision + dual link system HRP according to the manufacturer's instructions. The sections were counterstained with Mayer's hematoxylin and mounted in Faramount aqueous mounting medium (Dako). The immune-staining was evaluated by light photomicroscopy (Carl Zeiss, Weesp, The Netherland) using a high resolution camera (Canon G10, Japan).

For detection of β-catenin and active caspase-3, tissue sections were incubated with 10μg/ml of antibody for overnight at 4°C and appropriate secondary antibody labeled with FITC for 45 min at room temperature. To visualize the nuclei cells were fixed in Prolong gold antifade reagent with DAPI (Invitrogen). After mounting the specimens on slides with Vectashield, antigen distribution was examined under a Nikon Eclipse TE2000-S florescence microscope (Nikon Instrument INC, Melville, NY).

Mouse/rabbit isotype control antibodies (Abcam) were used at the same concentration as the primary antibodies and sections were incubated simultaneously with isotype control antibodies for all primary antibodies used.

For macrophage staining we used antibodies targeted to F4/80, ITGAX (CD11c) and MRC1 (CD206), which identify macrophages, M1 and M2 macrophage subtypes respectively (18, 35, 36). The Dako EnVision G-2 double stain system (Dako) was used to stain the frozen sections according to the manufacturer's instructions with slight modification. 1:200 and 1:25 dilutions were used for ITGAX and MRC1 (Abcam), respectively. The visualization of MRC1 and ITGAX was done by HRP using DAB chromogen and alkaline phosphatase using permanent red chromogen, respectively. Macrophage staining was also performed in reverse order to confirm the specificity. The number of macrophages was counted in at least ten randomly chosen areas per uterine section at 40X view. The numbers of animals were 4–6 for each group and six sections per animal were analyzed. Macrophage staining was also confirmed by immunofluorescence (same concentration of antibodies as for immunohistochemistry) using the method as described for active caspase-3.

The tissue immunostaining results were scored negative if no immunopositive tissue was present. The total score was based on the percentage of stained tissue and immunostaining intensity. The percentage of stained tissue and immunostaining intensity was calculated according to the method described in Teixeira et al., 2009 (37). Then, the immunostaining index score (ISIS) was generated by using the equation stained area score (SAS) multiplied by the immunostaining intensity score (IIS): (ISIS = SAS × IIS).

Protein extraction

For cytokine/chemokine assays uterus and placenta were homogenized in ice-cold 1X radioimmune precipitation assay (RIPA) buffer (Santa Cruz Biotechnology) containing protease and phosphatase inhibitor (Roche Applied science, Indianapolis, IN). Lysates were incubated on ice for 30 min and centrifuged at 10,000*xg* for 10 minutes at 4°C. Supernatant fluid was collected and used as a total cell lysates for protein assays. Protein concentration

was measured spectrophotometrically (Nanodrop 2000, Thermo Scientific, Hanover Park, IL) at A_{280}.

Caspase activity measurement

Activity of caspase-9, −8, −3 and −1 was measured using SensoLyte AFC Caspase Profiling Kit (AnaSpec, Inc., Fremont, CA) in total cell lysate from uterus (38) and assayed on fluorescence microplate reader, flurometer (Bio-Tek Instruments, Winooski, VT) as per the instruction provided by manufacture. Equal amounts of protein (50μg) from total cell lysates were used for the assay. Caspase activity was measured in relative fluorescence unit (RFU)/μg of protein. The assay was run with duplicates with n=4 in each group.

Western blot analysis

Equal amounts of protein (50μg) from total cell lysates were separated by 4–20% SDS-PAGE and blotted onto PVDF transfer membranes. The membranes were blocked at room temperature for 1 hour in 5% nonfat dry milk in TBS-T. Blots were incubated with the rabbit anti-a2NTD, rabbit anti-FAS, rabbit anti-FADD and rabbit anti-caspase-1 primary antibody overnight at 4°C and with appropriate secondary antibody for 1 hour at room temperature. Fluorescent blots were imaged on the Odyssey Infrared Imaging System (LI-COR Biosciences). After detection of signal for the target protein, membranes were re-probed for GAPDH. Each experiment was done twice in duplicate.

Cytokine/Chemokine bioassay

The secretion of a panel of mouse cytokine/chemokines and FasL was analyzed by Milliplex map kit (Millipore, St. Charles, MO) in the supernatant of RAW 264.7 cells and total cell lysates from uterus or placenta, and assayed on a MAGPIX instrument (Millipore) as per the instructions provided by manufacture. Equal amounts of protein (50μg) from total cell lysates were used for the assay. The assay was repeated three times with duplicates.

Statistical analysis

Continuous variables (e.g. relative mRNA levels) were assessed with Student's t-test or ANOVA or, when data were not normally distributed and two groups were compared, the Mann-Whitney U test.

Results

a2V expression decreases in PGN+poly(I:C) induced preterm labor

In order to test whether a2V plays a role in infection-induced preterm labor, a well-validated mouse model of infection-induced preterm labor using combined stimulation by bacterial and viral products was employed (7). The right uterine horn was injected with either PGN +poly(I:C) or saline on day 14.5 of pregnancy. Real-time PCR was performed in tissues harvested 8 hours after surgery. The mRNA expression of a2V was significantly decreased with PGN+poly(I:C) treatment in uterus, placenta and fetal membranes but not in the fetus (Fig. 1A–C, Supplemental Fig. 1A).

Immunohistochemistry correlated with the mRNA levels and showed that expression of a2V protein was decreased in both myometrium and decidua due to PGN+poly(I:C) treatment. Overall ISIS (immunostaining index score) of a2V in the uterus was significantly decreased after PGN+poly(I:C) treatment (ISIS=6.62±0.5) when compared to the respective control (ISIS=10.92±0.4, $p \leq 0.01$) (Fig. 1D, E), as it was in placenta following PGN+poly(I:C) (ISIS=7.7±0.4) compared to control (ISIS=10.70±0.3, $p \leq 0.01$) (Fig. 1D, F).

Using an antibody that detects the cleaved N-terminus domain of a2V protein (i.e., a2NTD), western blot was performed to evaluate cleavage of a2V protein in uterus and placenta of control and PGN+poly(I:C) treated animals. Compared with uterus and placenta from control animals, decreased levels of a2NTD were noted in the uterus and placenta from PGN +poly(I:C) treated animals (Fig. 1G). We also determined the mRNA expression of trophoblast development markers *Hbegf* and *Hox10* which remained same in control and PGN+poly(I:C) treated placenta (Supplemental Fig. 1B, 1C).

As seen with mRNA and protein localization, a2V was highly expressed in control uterus and placenta. This expression is required for normal spongiotrophoblast development and invasion. However in PGN+poly(I:C) treated uterus and placenta, a2V was significantly reduced, which could disturb the integrity and normal physiological function of decidual cells and spongiotrophoblast and lead to premature pregnancy loss. The resulting preterm labor in the PGN+poly(I:C) treated group was associated with lower density (ISIS) of a2V positive cells in decidua cells and spongiotrophoblast (Fig. 1E, 1F, Table1). Staining profile of the whole uteroplacental unit is shown with the demarcation of the different zones (Supplemental Fig. 2).

Decrease of a2V is associated with induction of iNOS and altered integrity of adherens junctions in PGN+poly(I:C) treated uterus and placenta

We observed that blocking of a2V by anti-a2V induces iNOS and TNF-α mRNA expression, and TNF-α secretion *in vitro*. Moreover, anti-a2V enhances PGN+poly(I:C) induced iNOS and TNF-α in comparison to respective controls (Supplemental Fig. 3A–C). It has been reported that blocking of V-ATPase induces iNOS expression (39). Here, in the mouse preterm labor model we show that the decrease of a2V in PGN+poly(I:C) treated animals is associated with the induction of iNOS mRNA in both uterus and placenta (Fig. 2A, 2B). The expression of iNOS protein was significantly increased in immunohistochemical analysis of both uterine decidual and mononuclear cells (Fig. 2C, 2D) and placental spongiotrophoblast (Fig. 2E, 2F) after PGN+poly(I:C) treatment compared to control.

NOS is structurally associated with cadherin/β-catenin/actin complex (40) and its activation is a key regulator of adherens junctions (41). Structural assessment of the uterus and placenta by immunolocalization of E-cadherin and N-cadherin revealed that E-cadherin and N-cadherin were localized on the plasma membrane of uterine decidual cells and placental spongiotrophoblast of the control group (Fig. 3A, 3C, 3E and 3G). However, in the PGN +poly(I:C) group, uterine decidual cells and placental spongiotrophoblast undergo a morphologic shift in the expression of membrane E-cadherin and N-cadherin, consistent with loss or internalization (Fig. 3B, 3D, 3F and 3H).

The extent to which the treatment with PGN+poly(I:C) affects other plasma membrane proteins is not known. Because other cell-adhesion molecules, such as β-catenin are associated with cadherins, we examined the membrane expression of β-catenin using immunofluorescence. Similar to cadherins, both the level of surface expression and the proportion of cells expressing surface β-catenin was low in PGN+poly(I:C) treated uterus and placenta (Fig. 3I–P). Isotype controls were also shown (Fig. 2G, 2H, Supplemental fig. 4A, 4B). These results suggest that disruption of a2V in the PGN+poly(I:C) treated uterus and placenta is associated with iNOS activation, which ultimately causes the weakening of adherens junctions among uterine decidual cells and placental spongiotrophoblast.

PGN+poly(I:C) induces apoptosis in the uterus and placenta via the extrinsic pathway

PGN+poly(I:C) treated uterus and placenta showed significant decrease in expression of a2V and increase in expression of iNOS mRNA and protein compared to control. The blocking of V-ATPase and activation of iNOS induces apoptosis in various cells (23, 25, 39). Therefore, we examined various apoptotic markers belonging to the extrinsic and intrinsic pathways of apoptosis in uterus and placenta during PGN+poly(I:C) induced preterm labor by immunohistochemistry. The immunolocalization of the pro-apoptotic marker Bax was significantly higher in control uterus compared to PGN+poly(I:C) treated uterus (Fig. 4A, B, M). However, no difference was observed in placental Bax expression (Fig. 5A, B, M).

The expression of the anti-apoptotic marker bcl2 was similar in uterus and placenta of both groups (Fig. 4C, D, N, 5C, D, N). The cleaved caspase-9 also remained unchanged in uterus and placenta of both groups (Fig. 4E, F, O, 5E, F, O). In control uterus some decidual cells had higher levels of cleaved caspase-9 (Fig. 4E, F). Cleaved caspase-8 (Fig. 4G, H, P, 5G, H, P) and caspase-3 (Fig. 4I–L, 5I–L) were significantly increased in the PGN+poly(I:C) treated uterus and placenta compared to control. Isotype controls were also shown (Fig. 2G, H, Supplemental fig. 4A, B). Activity of caspase-9,-8 and −3 was measured in uterus using fluorometry. Activity of caspase-9 remained same in both the groups while activity of caspase-8 and −3 was higher in PGN+poly(I:C) treated group as compared to control (Fig. 4Q) as shown by immunohistochemistry.

These data indicate that apoptosis induced by PGN+poly(I:C) treatment is regulated by the extrinsic pathway of apoptosis, as indicated by the increased activation of caspase-8 and caspase-3. To further verify that PGN+poly(I:C) induces apoptosis through the extrinsic pathway, the levels of death receptor Fas; its ligand, Fas L and FAS associated death domain protein (FADD) belonging to the extrinsic pathways of apoptosis were investigated in the uterus and placenta. Immunohistochemistry results showed that the expression levels of FAS (Fig. 6A–C, J–L), FasL (Fig. 6D–F, M–O) and FADD (Fig. 6G–I, P–R) were significantly increased in PGN+poly(I:C) treated uterus and placenta compared to control. Western blot analysis of Fas and FADD (Fig. 6S, U and V) and luminex assay of FasL (Fig. 6T) also confirmed the higher expression levels of FAS, FasL and FADD in PGN+poly(I:C) treated uterus and placenta compared to control. Isotype controls were also shown (Fig. 6W). These results further confirm that the apoptosis induced by PGN+poly(I:C) treatment occurs via the extrinsic pathway.

PGN+poly(I:C) induces upregulation of M2-like macrophage markers in uterus but not in placenta

Pro-inflammatory chemokines have been reported to associate with preterm birth (42). Therefore, we determined the expression of pro-inflammatory chemokine, Monocyte chemotactic protein-1 (MCP-1) in uterus and placenta of control and PGN+poly(I:C) treated groups. Its expression was significantly increased in uterus and placenta of PGN+poly(I:C) treated group with more robust expression in the PGN+poly(I:C) treated uterus (Fig. 7A and 10A, B). MCP-1 is capable of recruiting monocytes/macrophages into sites of inflammation, as well as stimulating the respiratory burst required for macrophage activation. MCP-1 transcripts and immuno-reactivity were expressed by uterine tissues (i.e., decidual cells and myometrium) and, thus, may participate in the process of labor (42). Macrophages are the cells responsible for phagocytosis and elimination of apoptotic cells and exhibit inflammatory response or express anti-inflammatory cytokines for the resolution of inflammation (43). Therefore we examined the markers associated with macrophage polarization during PGN+poly(I:C) induced preterm labor. F4/80 (general macrophage marker) was significantly increased in PGN+poly(I:C) treated uterus but remained

unchanged in placenta compared to controls (Fig. 7B). The mRNA expression of M1 macrophage markers CD11c remained unchanged in uterus and placenta of controls and PGN+poly(I:C) treated groups (Fig. 7C). However, mRNA expression of M2 macrophage markers Mrc1 (CD206), Arg1 and CD209a was significantly upregulated in PGN+poly(I:C) treated uterus compared to controls (Fig. 7D–F). In contrast, placental mRNA expression of Mrc1 was same in control and preterm labor groups (Fig. 7D) and Arg1 and CD209a were undetectable (Fig. 7E, F). These results indicate that M2 macrophage markers are increased in PGN+poly(I:C) treated uterus but not in placenta.

M1 and M2 polarization during preterm labor

We determined the distribution of M1 and M2-like macrophages in control and PGN +poly(I:C) treated uteri. The presence of macrophages in the uterus was confirmed by F4/80 localization by immunohistochemistry and immunofluorescence (Fig. 8A–B and 8C–F). The immunostaining result showed that the number of F4/80+ cells or uterine macrophages were increased in PGN+poly(I:C) treated uterus compared to the control uterus (Fig. 8M). Double immunostaining on serial sections for CD11c (brown, M1 macrophage marker) and CD206 (Mrc1, red, M2 macrophage marker) showed that macrophages in control uterus preferentially expressed CD11c (Fig. 8G) while those in PGN+poly(I:C) treated uterus expressed both CD11c and CD206 (Fig. 8H). To validate double immunostaining, serial sections were immunostained with reverse staining of CD11c (red) and CD206 (brown), yielding the same result (Fig. 8I, J). Isotype controls were also shown (Fig. 8K, L).

This result was also confirmed by the double-immunofluorescence staining of F4/80/CD11c and F4/80/CD206 in serial sections of uterus. In control uterus, few F4/80+ macrophages preferentially expressed CD11c (Fig. 9A–F). However, in PGN+poly(I:C) treated uterus ~ 85% F4/80+ macrophages expressed both CD11c and CD206 (Fig. 9G–L). Isotype controls are also shown (Supplemental fig. 4C–H). These results suggest that in the PGN+poly(I:C) treated uterus, the number of F4/80+ macrophages were increased and these macrophages shift towards the double positive for CD11c and CD206 (Fig. 8M).

M1 and M2 macrophage associated cytokines during preterm labor

To further determine M1 and M2 polarization, the levels of M1 macrophage-associated cytokines (IFN-γ, IL-1β, IL-6, IL-12p70 and TNF-α), M2 macrophage-associated cytokine (IL-10), chemokines (G-CSF, GM-CSF, MCP1 and MIP-1α), and other cytokines IL-2 and LIF by the luminex assay. M1 macrophage-associated proinflammatory cytokines were significantly elevated in PGN+poly(I:C) treated uterus (Fig. 10A) and placenta (Fig. 10B) compared to control. The M2 macrophage-associated anti-inflammatory cytokine, IL-10 was significantly increased in PGN+poly(I:C) treated uterus (Fig. 10A) but not in placenta (Fig. 10B). The chemokines were significantly elevated in PGN+poly(I:C) treated uterus (Fig. 10A) and placenta (Fig. 10B) compared to the control. There was no change in IL-2 level. LIF was significantly increased in PGN+poly(I:C) treated uterus and placenta. These observations indicate that during PGN+poly(I:C) induced preterm labor both M1 and M2 macrophage-associated cytokines are increased in the uterus while few M1 macrophage-associated cytokines are increased in the placenta.

Inflammasome activation during preterm labor

a2V functions as an ATPase on the cell surface and prevents the DAMP (danger associated molecular pattern) adenosine triphosphate (ATP) from activating the inflammasomes (44). ATP can trigger the activation of NLRP3 inflammasome in response to pathogen-associated molecular patterns (PAMPs), such as PGN and LPS (45). It stimulates the caspase-1 dependent cleavage and secretion of IL-1β from cells stimulated with PAMPs (46). We observed low expression of a2V in PGN+poly(I:C) treated uterus; therefore, we examined

the total ATP concentration in control and PGN+poly(I:C) treated uterus. The total ATP concentration was significantly increased in PGN+poly(I:C) treated uterus when compared to control (Fig. 11A). We further examined the mRNA expression of Nlrp3 and caspase-1 which was significantly increased in the PGN+poly(I:C) treated uterus compared to control (Fig. 11B, 11C). Cleavage of pro-caspase-1 into active caspase-1 and activity of caspase-1 was also increased significantly in the PGN+poly(I:C) treated uterus compared to control (Fig. 11D, E). *Nlrp3* and *caspase-1* gene expression and cleavage of pro-caspase-1 were undetectable in placenta. These results demonstrate the activation of inflammasomes in response to PGN+poly(I:C) treatment.

Discussion

The internal acidification of intracellular compartments such as lysosomes, endosomes, Golgi complexes, and secretary granules has been suggested to be critical to cell survival and function (47). V-ATPase plays a critical role in the maintenance of intracellular compartments and extracellular pH by pumping protons to the extracellular environment. This low acidic pH triggers proteases which results in the dissolution of extracellular matrix. This process is well known for the contribution of tumor invasion and dissemination (48). We have shown that placental a2V-ATPase (a2V) plays a critical role in the development of trophoblast and its invasion in normal pregnancy (17). On the other hand, decreased placental a2V is associated with upregulation of proinflammatory cytokines such IL-1β, TNF-α, etc during LPS-induced abortion (17). Other investigators have described the fundamental role of V-ATPase during cytokine trafficking and secretion (49–51). Our previous studies showed that a2NTD signaling of a2V participates in the induction of immune tolerogenic state during tumorigenesis (52, 53).

In the present study we report that during PGN+poly(I:C) induced preterm labor a2V expression and cleaved a2NTD level were significantly reduced in the uterus and placenta. This decreased a2V expression might halt the further development of placental trophoblast and hinders the production of one of a2V's main target products, cleaved a2NTD, which is in part responsible for the maintenance of immune tolerogenic state (52). Loss of this tolerance may manifest preterm labor.

NOS is structurally associated with the cadherin/β-catenin/actin complex (40) and its activation is a key regulator of the adherens junction (41). Several reports have suggested that V-ATPase inhibitors prevent the cell growth and survival through the iNOS via NO production which is a potent inducer of apoptosis in various cell types (39, 54–56). We observed that the decreased expression of a2V is allied with upregulation of iNOS in both myeloid and non-myeloid cells of PGN+poly(I:C) treated uterus and placenta. Our *in vitro* data also showed that blocking of a2V by anti-a2V is directly associated with the induction of iNOS gene expression. It is reported that upregulation of iNOS is associated with disruption or opening of cell-to-cell contacts and induction of apoptosis (40, 41, 57). Our data showed that adherens junctions in uterine decidua and placental trophoblast is disrupted, as evidenced by the disassembly of E-cadherin, N-cadherin and β-catenin during PGN+poly(I:C) induced preterm labor. We suggest that down-regulation of a2V in the PGN +poly(I:C) treated uterus and placenta is associated with iNOS activation, which ultimately causes the weakening of adherens junctions among uterine decidual cells and placental spongiotrophoblasts.

A V-ATPase inhibitor (bafilomycin A1) induces apoptosis in various mammalian cells lines (22–24). We showed that apoptosis induced by PGN+poly(I:C) treatment is regulated by the extrinsic pathway of apoptosis as indicated by the increased activation of caspase-8 followed by caspase-3. Further investigation revealed that PGN+poly(I:C) can also activate the FAS/

FasL/FADD death pathway in the uterus and placenta. It is reported that blocking V-ATPase enhances TNF-α induced DNA fragmentation and activation of caspase-8 (58). Our *in vitro* data showed that PGN+poly(I:C) induced TNF-α and iNOS was significantly enhanced in presence of anti-a2V. We have also shown that in the PGN+poly(I:C) treated uterus and placenta, TNF-α and iNOS were significantly upregulated. Therefore, it is possible that in the presence of PGN+poly(I:C), which itself induces the upregulation of TNF-α and iNOS, this upregulation might be enhanced because of the decreased levels of a2V in uterus and in placenta undergoing preterm labor. Interaction of TNF-α with its receptor (TNF-R1) induces recruitment of the death domain-containing cytosolic adapter proteins TRADD (TNF-R1-associated death domain) and FADD (Fas-associated death domain), and pro-caspase-8, which triggers the caspase activation cascade and apoptosis (59). Thus, our results shows that the activation of the extrinsic apoptotic pathway might be associated with the decreased expression of a2V and enhanced Fas signaling and levels of iNOS and TNF-α in the PGN +poly(I:C) treated uterus and placenta.

Cell death by apoptosis may trigger inflammation and also suppresses inflammatory responses (43). Intracellular mechanisms underlying inflammatory responses induced by PGN+poly(I:C) involve direct activation of NF-κB or via degradation of IκBα in macrophage cell line (8). The inflammatory response induced by PGN+poly(I:C) also involves induction of a second signaling event downstream of TLR activation is phosphorylation of extracellular signal-regulated kinases (ERK)-1 and ERK-2, via PGN +poly(I:C) that play important role in cell proliferation, apoptosis and inflammation (3, 8).

Here we identify apoptosis and the innate immune response as dual pathogenic factors in the uterus and placenta undergoing preterm labor during a double hit of infection initiated by PGN+poly(I:C). The simultaneous activation of apoptosis and a specific innate immune response represents a critical pathogenic step in the induction preterm labor. We showed that in the PGN+poly(I:C) treated uterus, the number of macrophages (F4/80+) were increased. Gonzalez et al., 2011 demonstrated the increased infiltration of macrophages in mice that deliver preterm in response to LPS treatment. Depletion of F4/80+ macrophages prevented cervical remodeling and preterm delivery in LPS-treated mice (60). Our macrophage phenotypes study showed that these increased macrophages (F4/80+) were double-positive for CD11c and CD206. We could not identify separate populations of M1 (CD11c+) or M2 (CD206) macrophages in the PGN+poly(I:C) treated uterus although uterine macrophages in control animals were mainly M1-like (CD11c+). We propose that the deployment of double positive (CD11c+ and CD206+) macrophages and their respective cytokines responses (both M1 and M2 cytokines) may contribute to recruitment and activation of innate immune defenses when uterine cell death occurs at infected or inflamed sites. We further propose that this combinatorial pro and anti-inflammatory effect of double-positive macrophages on the uterine apoptotic cells is critical for the clearance of dying cells and then rapidly abetting the resolution of inflammation.

Previously we have shown that under chronic pathologic conditions like LPS-induced abortion, placental a2V is decreased and linked with upregulation of proinflammatory cytokines such IL-1β, TNF-α, Mcp1, etc (17). Derks et al., 2004 have shown that the secretion of IL1-β from human monocytes was enhanced with anti-a2V in combination with exogenous ATP. It has been previously shown that a2V expression occurs on the cell surface, where it functions as an ATPase and prevents extracellular ATP from activating the inflammasome through the P2X7 channel (44). ATP binding to P2X7 causes the efflux of potassium ions and activation of inflammasomes (61). Our study showed that PGN +poly(I:C) treatment activates caspase-1 via Nlrp3 inflammasome, though it is possibile that there was a contribution from decreased a2V activity leading to elevated ATP levels, which activate the inflammasome through P2X7 channel. The over-expression and activation of

caspase-1 during a lethal response to LPS is a crucial mediator of apoptosis and maturation of the cytokines IL-1 and IL-18 (62, 63). Here we showed that PGN+poly(I:C) exposure also resulted in over-expression and activation of caspase-1 which could induce pyroptosis and lead to preterm labor.

Therefore, the double hit of PGN and poly(I:C) induces preterm labor in the murine model via simultaneous activation of apoptosis and inflammatory processes. a2V might be a bridge linking these apoptotic and inflammatory processes, and may be a useful therapeutic target for preterm labor.

Supplementary Material

Refer to Web version on PubMed Central for supplementary material.

Acknowledgments

Grant support: Funded in part by NIH (#1R01 HD056118 and 3R01HD056118-03S1), the March of Dimes Birth Defects Foundation (#21-FY10-202), the Clinical Immunology, Rosalind Franklin University of Medicine and Science, North Chicago, IL, USA.

Abbreviations

a2V	a2 isoform of V-ATPase
PGN	Peptidoglycan
(poly(I:C)	polyinosinic:cytidylic acid
IU	Intrauterine

References

1. Agrawal V, Hirsch E. Intrauterine infection and preterm labor. Semin Fetal Neonatal Med. 2011; 17:12–19. [PubMed: 21944863]
2. Lamont RF. Infection in the prediction and antibiotics in the prevention of spontaneous preterm labour and preterm birth. Bjog. 2003; 20(110 Suppl):71–75. [PubMed: 12763116]
3. Akira S, Takeda K. Toll-like receptor signalling. Nat Rev Immunol. 2004; 4:499–511. [PubMed: 15229469]
4. Thaxton JE, Nevers TA, Sharma S. TLR-mediated preterm birth in response to pathogenic agents. Infect Dis Obstet Gynecol. 2010 2010.
5. Li L, Kang J, Lei W. Role of Toll-like receptor 4 in inflammation-induced preterm delivery. Molecular human reproduction. 2010; 16:267–272. [PubMed: 19995880]
6. Koga K, Aldo PB, Mor G. Toll-like receptors and pregnancy: trophoblast as modulators of the immune response. J Obstet Gynaecol Res. 2009; 35:191–202. [PubMed: 19335792]
7. Ilievski V, Hirsch E. Synergy between viral and bacterial toll-like receptors leads to amplification of inflammatory responses and preterm labor in the mouse. Biol Reprod. 2010; 83:767–773. [PubMed: 20650880]
8. Agrawal V, Smart K, Jilling T, Hirsch E. Surfactant Protein (SP)-A Suppresses Preterm Delivery and Inflammation via TLR2. PloS one. 2013; 8:e63990. [PubMed: 23700442]
9. Cardenas I, Means RE, Aldo P, Koga K, Lang SM, Booth CJ, Manzur A, Oyarzun E, Romero R, Mor G. Viral infection of the placenta leads to fetal inflammation and sensitization to bacterial products predisposing to preterm labor. J Immunol. 2010; 185:1248–1257. [PubMed: 20554966]
10. Cardenas I, Mor G, Aldo P, Lang SM, Stabach P, Sharp A, Romero R, Mazaki-Tovi S, Gervasi M, Means RE. Placental viral infection sensitizes to endotoxin-induced pre-term labor: a double hit hypothesis. Am J Reprod Immunol. 2011; 65:110–117. [PubMed: 20712808]

11. Trinchieri G, Sher A. Cooperation of Toll-like receptor signals in innate immune defence. Nat Rev Immunol. 2007; 7:179–190. [PubMed: 17318230]
12. Aksoy E, Zouain CS, Vanhoutte F, Fontaine J, Pavelka N, Thieblemont N, Willems F, Ricciardi-Castagnoli P, Goldman M, Capron M, Ryffel B, Trottein F. Double-stranded RNAs from the helminth parasite Schistosoma activate TLR3 in dendritic cells. J Biol Chem. 2005; 280:277–283. [PubMed: 15519998]
13. Bosch AA, Biesbroek G, Trzcinski K, Sanders EA, Bogaert D. Viral and bacterial interactions in the upper respiratory tract. PLoS pathogens. 2013; 9:e1003057. [PubMed: 23326226]
14. Park JS, Svetkauskaite D, He Q, Kim JY, Strassheim D, Ishizaka A, Abraham E. Involvement of toll-like receptors 2 and 4 in cellular activation by high mobility group box 1 protein. J Biol Chem. 2004; 279:7370–7377. [PubMed: 14660645]
15. Smiley ST, King JA, Hancock WW. Fibrinogen stimulates macrophage chemokine secretion through toll-like receptor 4. J Immunol. 2001; 167:2887–2894. [PubMed: 11509636]
16. Ntrivalas E, Gilman-Sachs A, Kwak-Kim J, Beaman K. The N-terminus domain of the a2 isoform of vacuolar ATPase can regulate interleukin-1beta production from mononuclear cells in co-culture with JEG-3 choriocarcinoma cells. Am J Reprod Immunol. 2007; 57:201–209. [PubMed: 17295899]
17. Jaiswal MK, Gilman-Sachs A, Chaouat G, Beaman KD. Placental ATPase expression is a link between multiple causes of spontaneous abortion in mice. Biol Reprod. 2011; 85:626–634. [PubMed: 21593477]
18. Jaiswal MK, Mallers TM, Larsen B, Kwak-Kim J, Chaouat G, Gilman-Sachs A, Beaman KD. V-ATPase upregulation during early pregnancy: a possible link to establishment of an inflammatory response during preimplantation period of pregnancy. Reproduction. 2012; 143:713–725. [PubMed: 22454532]
19. Ntrivalas E, Levine R, Kwong C, Gilman-Sachs A, Beaman K. The a2 isoform of vacuolar ATPase is a modulator of implantation and feto-maternal immune tolerance in early pregnancy. J Reprod Immunol. 2010; 85:106–111. [PubMed: 20036779]
20. Skinner MA, MacLaren LA, Wildeman AG. Stage-dependent redistribution of the V-ATPase during bovine implantation. J Histochem Cytochem. 1999; 47:1247–1254. [PubMed: 10490453]
21. Nishihara T, Akifusa S, Koseki T, Kato S, Muro M, Hanada N. Specific inhibitors of vacuolar type H(+)-ATPases induce apoptotic cell death. Biochem Biophys Res Commun. 1995; 212:255–262. [PubMed: 7612014]
22. Bowman EJ, Siebers A, Altendorf K. Bafilomycins: a class of inhibitors of membrane ATPases from microorganisms, animal cells, and plant cells. Proc Natl Acad Sci U S A. 1988; 85:7972–7976. [PubMed: 2973058]
23. Ohta T, Arakawa H, Futagami F, Fushida S, Kitagawa H, Kayahara M, Nagakawa T, Miwa K, Kurashima K, Numata M, Kitamura Y, Terada T, Ohkuma S. Bafilomycin A1 induces apoptosis in the human pancreatic cancer cell line Capan-1. J Pathol. 1998; 185:324–330. [PubMed: 9771488]
24. Xu J, Feng HT, Wang C, Yip KH, Pavlos N, Papadimitriou JM, Wood D, Zheng MH. Effects of Bafilomycin A1: an inhibitor of vacuolar H (+)-ATPases on endocytosis and apoptosis in RAW cells and RAW cell-derived osteoclasts. J Cell Biochem. 2003; 88:1256–1264. [PubMed: 12647307]
25. Boomer JS, Lee GW, Givens TS, Gilman-Sachs A, Beaman KD. Regeneration and tolerance factor's potential role in T-cell activation and apoptosis. Hum Immunol. 2000; 61:959–971. [PubMed: 11082509]
26. Green DR. Apoptotic pathways: paper wraps stone blunts scissors. Cell. 2000; 102:1–4. [PubMed: 10929706]
27. Adams JM, Cory S. The Bcl-2 protein family: arbiters of cell survival. Science. 1998; 281:1322–1326. [PubMed: 9735050]
28. Hengartner MO. The biochemistry of apoptosis. Nature. 2000; 407:770–776. [PubMed: 11048727]
29. Nagata S, Golstein P. The Fas death factor. Science. 1995; 267:1449–1456. [PubMed: 7533326]
30. Lee J, Richburg JH, Younkin SC, Boekelheide K. The Fas system is a key regulator of germ cell apoptosis in the testis. Endocrinology. 1997; 138:2081–2088. [PubMed: 9112408]

31. Boomer JS, Derks RA, Lee GW, DuChateau BK, Gilman-Sachs A, Beaman KD. Regeneration and tolerance factor is expressed during T-lymphocyte activation and plays a role in apoptosis. Hum Immunol. 2001; 62:577–588. [PubMed: 11390032]
32. Mussalli GM, Blanchard R, Brunnert SR, Hirsch E. Inflammatory cytokines in a murine model of infection-induced preterm labor: cause or effect? J Soc Gynecol Investig. 1999; 6:188–195.
33. Hirsch E, Saotome I, Hirsh D. A model of intrauterine infection and preterm delivery in mice. Am J Obstet Gynecol. 1995; 172:1598–1603. [PubMed: 7538729]
34. Elovitz MA, Wang Z, Chien EK, Rychlik DF, Phillippe M. A new model for inflammation-induced preterm birth: the role of platelet-activating factor and Toll-like receptor-4. Am J Pathol. 2003; 163:2103–2111. [PubMed: 14578208]
35. Fujisaka S, Usui I, Bukhari A, Ikutani M, Oya T, Kanatani Y, Tsuneyama K, Nagai Y, Takatsu K, Urakaze M, Kobayashi M, Tobe K. Regulatory mechanisms for adipose tissue M1 and M2 macrophages in diet-induced obese mice. Diabetes. 2009; 58:2574–2582. [PubMed: 19690061]
36. Aron-Wisnewsky J, Tordjman J, Poitou C, Darakhshan F, Hugol D, Basdevant A, Aissat A, Guerre-Millo M, Clement K. Human adipose tissue macrophages: m1 and m2 cell surface markers in subcutaneous and omental depots and after weight loss. J Clin Endocrinol Metab. 2009; 94:4619–4623. [PubMed: 19837929]
37. Teixeira Gomes RC, Verna C, Nader HB, dos Santos Simoes R, Dreyfuss JL, Martins JR, Baracat EC, de Jesus Simoes M, Soares JM Jr. Concentration and distribution of hyaluronic acid in mouse uterus throughout the estrous cycle. Fertil Steril. 2009; 92:785–792. [PubMed: 18930192]
38. Thornberry NA, Lazebnik Y. Caspases: enemies within. Science. 1998; 281:1312–1316. [PubMed: 9721091]
39. Hong J, Nakano Y, Yokomakura A, Ishihara K, Kim S, Kang YS, Ohuchi K. Nitric oxide production by the vacuolar-type (H+)-ATPase inhibitors bafilomycin A1 and concanamycin A and its possible role in apoptosis in RAW 264.7 cells. J Pharmacol Exp Ther. 2006; 319:672–681. [PubMed: 16895977]
40. Lee NP, Mruk DD, Wong CH, Cheng CY. Regulation of Sertoli-germ cell adherens junction dynamics in the testis via the nitric oxide synthase (NOS)/cGMP/protein kinase G (PRKG)/beta-catenin (CATNB) signaling pathway: an in vitro and in vivo study. Biol Reprod. 2005; 73:458–471. [PubMed: 15858215]
41. Gonzalez D, Rojas A, Herrera MB, Conlan RS. iNOS activation regulates beta-catenin association with its partners in endothelial cells. PLoS One. 2012; 7:e52964. [PubMed: 23285236]
42. Esplin MS, Romero R, Chaiworapongsa T, Kim YM, Edwin S, Gomez R, Mazor M, Adashi EY. Monocyte chemotactic protein-1 is increased in the amniotic fluid of women who deliver preterm in the presence or absence of intra-amniotic infection. The journal of maternal-fetal & neonatal medicine : the official journal of the European Association of Perinatal Medicine, the Federation of Asia and Oceania Perinatal Societies, the International Society of Perinatal Obstet. 2005; 17:365–373.
43. Lucas M, Stuart LM, Savill J, Lacy-Hulbert A. Apoptotic cells and innate immune stimuli combine to regulate macrophage cytokine secretion. J Immunol. 2003; 171:2610–2615. [PubMed: 12928413]
44. Derks R, Beaman K. Regeneration and tolerance factor modulates the effect of adenosine triphosphate-induced interleukin 1 beta secretion in human macrophages. Hum Immunol. 2004; 65:676–682. [PubMed: 15301855]
45. Stout-Delgado HW, Vaughan SE, Shirali AC, Jaramillo RJ, Harrod KS. Impaired NLRP3 inflammasome function in elderly mice during influenza infection is rescued by treatment with nigericin. J Immunol. 2012; 188:2815–2824. [PubMed: 22327078]
46. Mariathasan S, Weiss DS, Newton K, McBride J, O'Rourke K, Roose-Girma M, Lee WP, Weinrauch Y, Monack DM, Dixit VM. Cryopyrin activates the inflammasome in response to toxins and ATP. Nature. 2006; 440:228–232. [PubMed: 16407890]
47. Wieczorek H, Brown D, Grinstein S, Ehrenfeld J, Harvey WR. Animal plasma membrane energization by proton-motive V-ATPases. Bioessays. 1999; 21:637–648. [PubMed: 10440860]
48. Nishi T, Forgac M. The vacuolar (H+)-ATPases--nature's most versatile proton pumps. Nat Rev Mol Cell Biol. 2002; 3:94–103. [PubMed: 11836511]

49. Martinez-Zaguilan R, Seftor EA, Seftor RE, Chu YW, Gillies RJ, Hendrix MJ. Acidic pH enhances the invasive behavior of human melanoma cells. Clin Exp Metastasis. 1996; 14:176–186. [PubMed: 8605731]
50. Coakley RJ, Taggart C, McElvaney NG, O'Neill SJ. Cytosolic pH and the inflammatory microenvironment modulate cell death in human neutrophils after phagocytosis. Blood. 2002; 100:3383–3391. [PubMed: 12384441]
51. Hinoki A, Yoshimura K, Fujita K, Akita M, Ikeda R, Nagashima M, Nomura M, Satomi A. Suppression of proinflammatory cytokine production in macrophages by lansoprazole. Pediatr Surg Int. 2006; 22:915–923. [PubMed: 16932910]
52. Kwong C, Gilman-Sachs A, Beaman K. Tumor-associated a2 vacuolar ATPase acts as a key mediator of cancer-related inflammation by inducing pro-tumorigenic properties in monocytes. J Immunol. 2011; 186:1781–1789. [PubMed: 21178005]
53. Kwong C, Gilman-Sachs A, Beaman K. An independent endocytic pathway stimulates different monocyte subsets by the a2 N-terminus domain of vacuolar-ATPase. Oncoimmunology. 2013; 2:e22978. [PubMed: 23483532]
54. Shimaoka M, Iida T, Ohara A, Taenaka N, Mashimo T, Honda T, Yoshiya I. NOC, a nitric-oxide-releasing compound, induces dose dependent apoptosis in macrophages. Biochem Biophys Res Commun. 1995; 209:519–526. [PubMed: 7733920]
55. Lincoln TM, Cornwell TL, Komalavilas P, Boerth N. Cyclic GMP-dependent protein kinase in nitric oxide signaling. Methods Enzymol. 1996; 269:149–166. [PubMed: 8791645]
56. Leist M, Volbracht C, Kuhnle S, Fava E, Ferrando-May E, Nicotera P. Caspase-mediated apoptosis in neuronal excitotoxicity triggered by nitric oxide. Mol Med. 1997; 3:750–764. [PubMed: 9407551]
57. Bandino A, Compagnone A, Bravoco V, Cravanzola C, Lomartire A, Rossetto C, Novo E, Cannito S, Valfre di Bonzo L, Zamara E, Autelli R, Parola M, Colombatto S. Beta-catenin triggers nuclear factor kappaB-dependent up-regulation of hepatocyte inducible nitric oxide synthase. Int J Biochem Cell Biol. 2008; 40:1861–1871. [PubMed: 18343708]
58. Han J, Sridevi P, Ramirez M, Ludwig KJ, Wang JY. beta-Catenin-dependent lysosomal targeting of internalized tumor necrosis factor-alpha suppresses caspase-8 activation in apoptosis-resistant colon cancer cells. Mol Biol Cell. 2013; 24:465–473. [PubMed: 23264463]
59. Ikner A, Ashkenazi A. TWEAK induces apoptosis through a death-signaling complex comprising receptor-interacting protein 1 (RIP1), Fas-associated death domain (FADD), and caspase-8. J Biol Chem. 2011; 286:21546–21554. [PubMed: 21525013]
60. Gonzalez JM, Franzke CW, Yang F, Romero R, Girardi G. Complement activation triggers metalloproteinases release inducing cervical remodeling and preterm birth in mice. Am J Pathol. 2011; 179:838–849. [PubMed: 21801872]
61. Kahlenberg JM, Dubyak GR. Mechanisms of caspase-1 activation by P2X7 receptor-mediated K+ release. Am J Physiol Cell Physiol. 2004; 286:C1100–C1108. [PubMed: 15075209]
62. Docke WD, Randow F, Syrbe U, Krausch D, Asadullah K, Reinke P, Volk HD, Kox W. Monocyte deactivation in septic patients: restoration by IFN-gamma treatment. Nat Med. 1997; 3:678–681. [PubMed: 9176497]
63. Sakao Y, Takeda K, Tsutsui H, Kaisho T, Nomura F, Okamura H, Nakanishi K, Akira S. IL-18-deficient mice are resistant to endotoxin-induced liver injury but highly susceptible to endotoxin shock. Int Immunol. 1999; 11:471–480. [PubMed: 10221659]

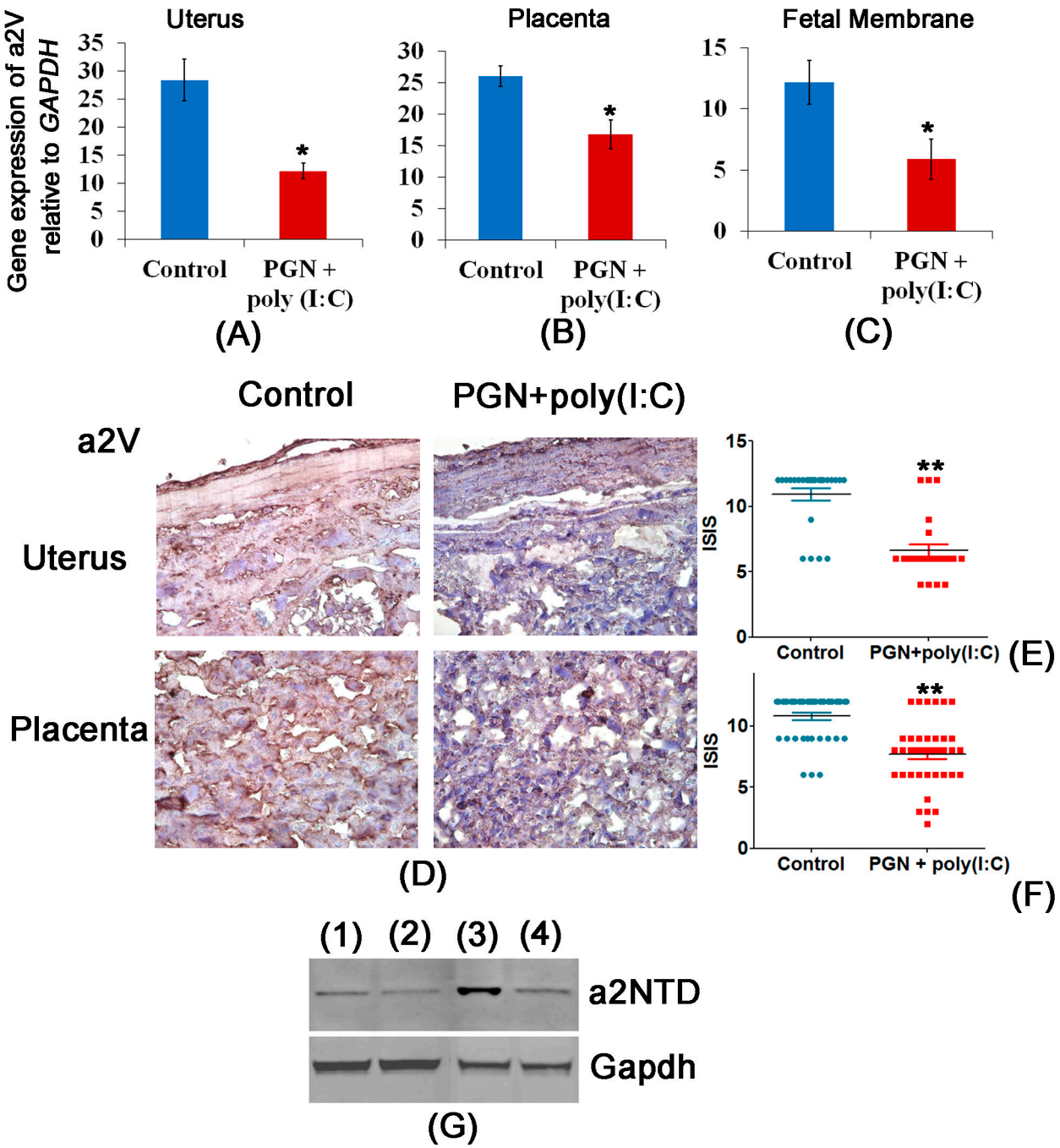

Figure 1. Expression of a2V is decreased in PGN+poly(I:C) induced preterm labor

Panels A, B and C show expression of *a2V* mRNA in uterus, placenta and fetal membrane recovered from control and PGN+poly(I:C) treated groups. Panel D shows the distribution of a2V protein, panels E and F show the immunostaining index score [(ISIS) = Stained area score (SAS) X Immunostaining intensity score (IIS)] of a2V in uterus and placenta recovered from control and PGN+poly(I:C) treated groups. Panel G shows the level of cleaved N-terminus domain of a2V i.e., a2NTD in uterus (lane 1) control and (lane 2) PGN +poly(I:C) treatment; and in placenta (lane 3) control and (lane 4) PGN+poly(I:C) treatment. N=6–11 each group. Six sections per animal were analyzed. Error bars=±SEM. *P≤0.05, **P≤0.01 Significant difference vs respective control. Original magnification: 400X.

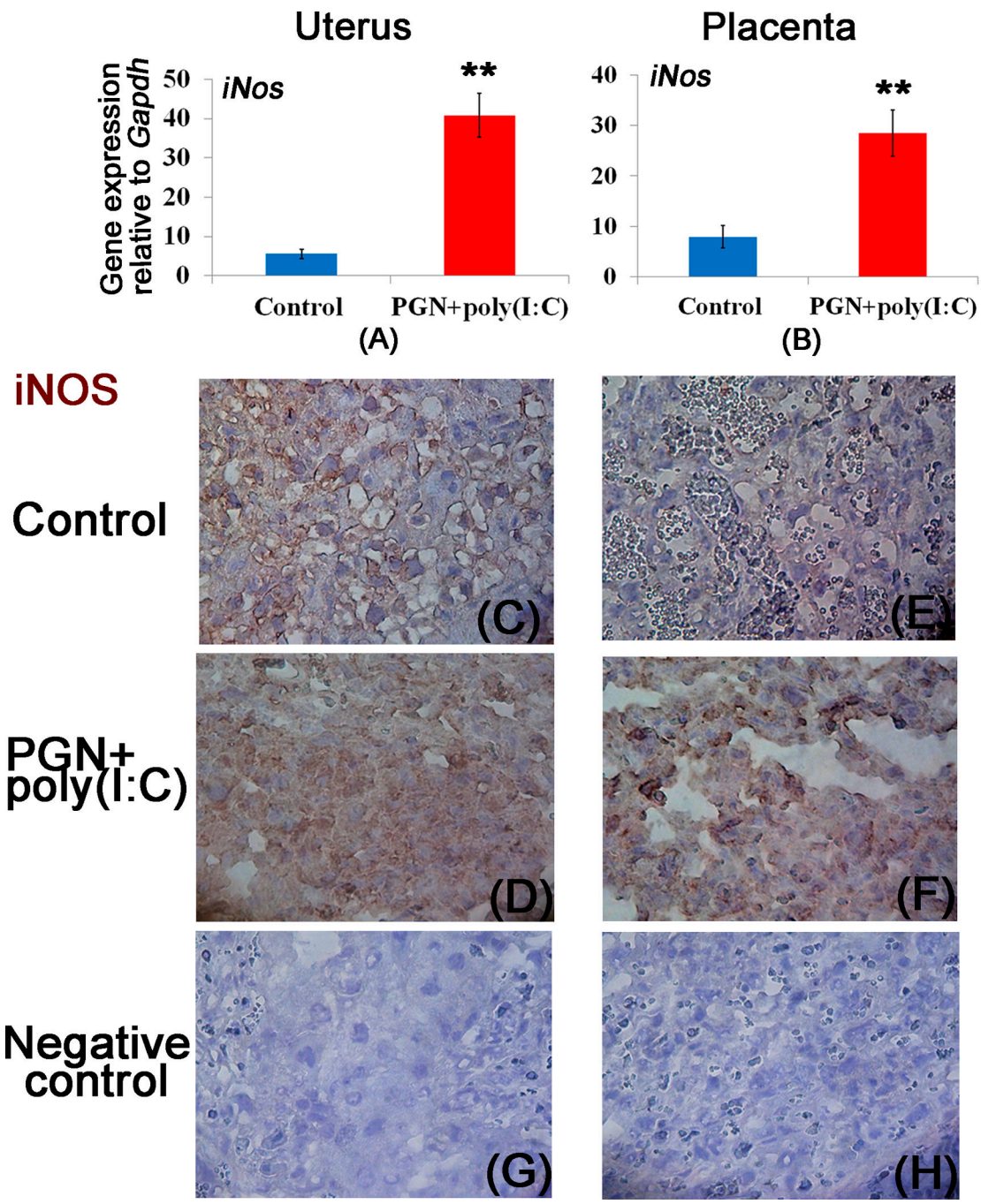

Figure 2. Decrease of a2V is associated with induction of iNOS

Panels A and B show mRNA expression of iNOS; panels C–D and E–F show immunolocalization of iNOS in the uterus and placenta recovered from the control and PGN +poly(I:C) treated groups, respectively. Panels G and H show the staining with isotype control antibodies for mouse IgG and rabbit IgG respectively. N=6–11 each group. Error bars= ±SEM. **P≤0.01 Significant difference vs respective control. Six sections per animal were analyzed. Original magnification: 400X.

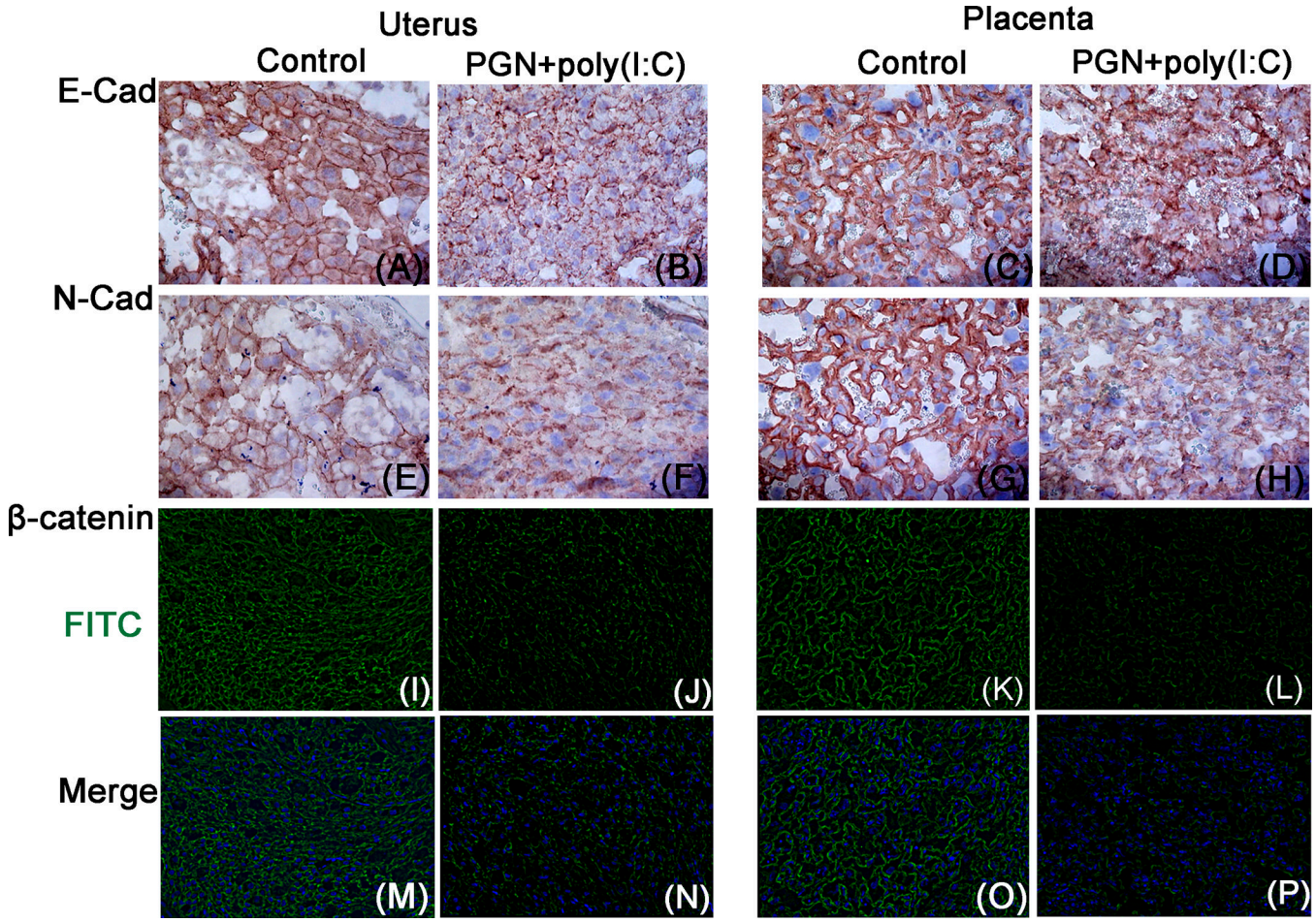

Figure 3. Loosening of adherens junctions in PGN+poly(I:C) treated uterus and placenta

Immunolocalization of E-cadherins, panel A–B and C–D; N-cadherins, panel E–F and G–H (Original magnification: 400X); β-catenin, panel I–J and K–L in the uterus and placenta recovered from the control and PGN+poly(I:C) treated groups, respectively. Panels M–P show the merge images (DAPI nuclear stain (blue), merged with FITC (stain for β-catenin)) for I–L, respectively. Original magnification: 200X. N=6 each group and six sections per animal were analyzed.

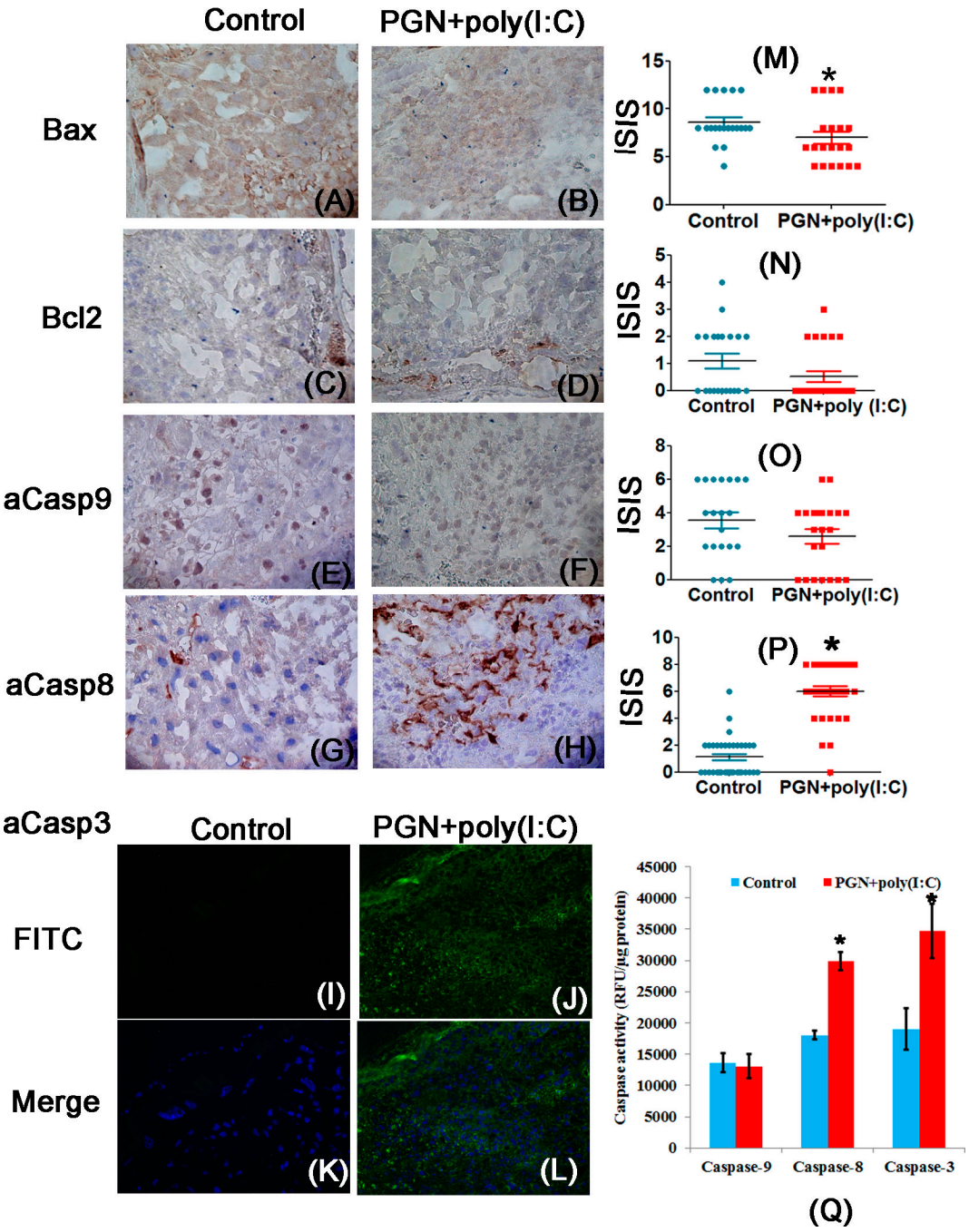

Figure 4. PGN+poly(I:C) induces apoptosis in the uterus via the extrinsic pathway

Immunolocalization of Bax, panel A and B; Bcl2, panel C and D; active caspase-9, panel E and F; active caspase-8, panel G and H; active caspase-3, panel I and J in uterus recovered from the control and PGN+poly(I:C) treated groups. Panel K and L are merged images (DAPI nuclear stain (blue), merged with FITC (stain for activated caspase-3)). Panels M, N, O and P show the immunostaining index score (ISIS) of Bax, Bcl2, active caspase-9 and active caspase-8 in the uterus recovered from control and PGN+poly(I:C) treated groups. Panel Q shows the caspases activity. N=4–6 each group and six sections per animal were analyzed. Error bars=±SEM. *P≤0.05 Significant difference vs respective control. Original magnification: 400X.

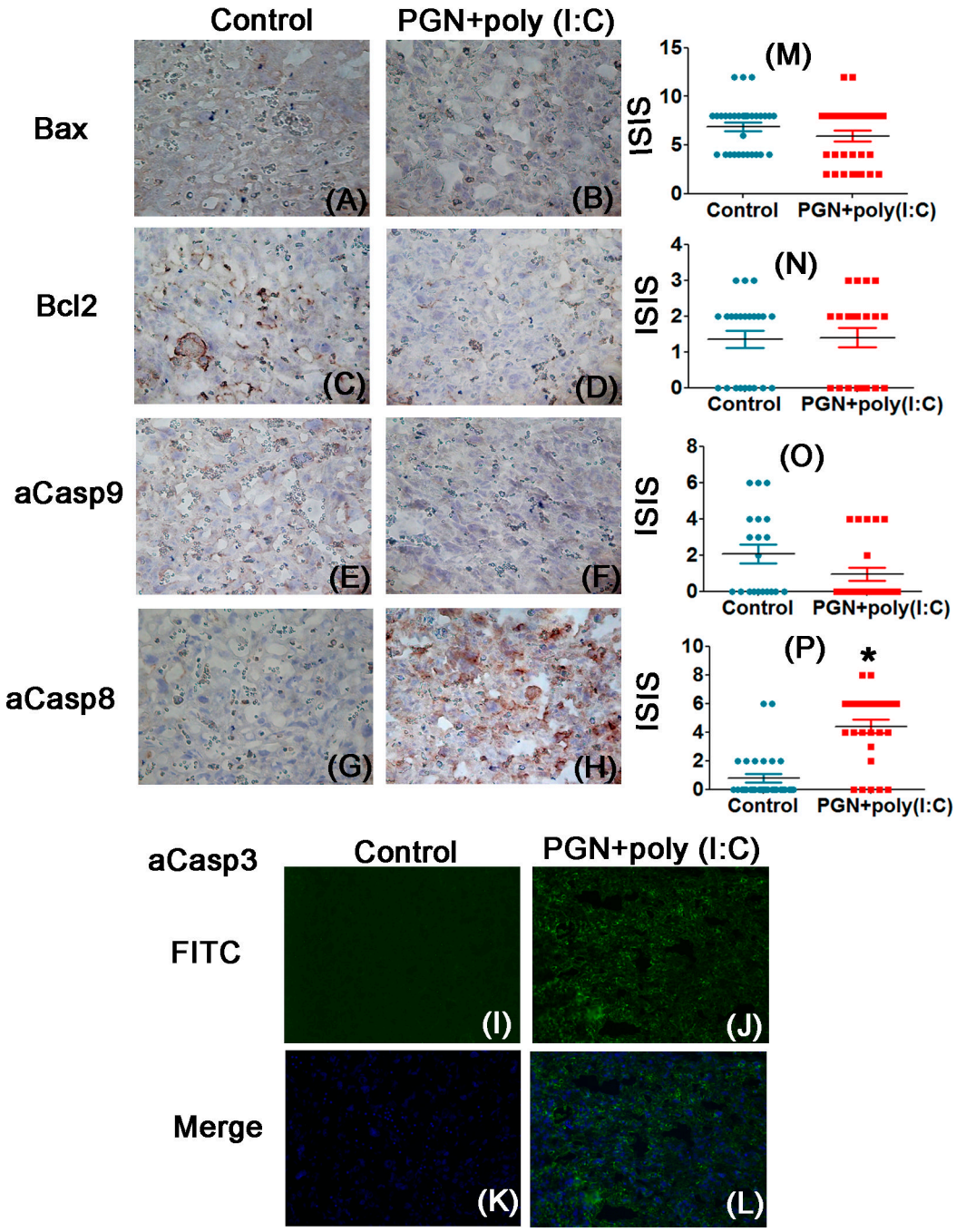

Figure 5. PGN+poly(I:C) induces apoptosis in the placenta via the extrinsic pathway

Immunolocalization of Bax, panel A and B; Bcl2, panel C and D; active caspase-9, panel E and F; active caspase-8, panel G and H; active caspase-3, panel I and J in placenta recovered from the control and PGN+poly(I:C) treated groups. Panel K and L are merged images (DAPI nuclear stain (blue), merged with FITC (stain for activated caspase-3)). Panels M, N, O and P show the immunostaining index score (ISIS) of Bax, Bcl2, active caspase-9 and active caspase-8 in placentas recovered from control and PGN+poly(I:C) treated groups. N=6 each group and six sections per animal were analyzed. Error bars= ±SEM. *P≤0.05 Significant difference vs respective control. Original magnification: 400X.

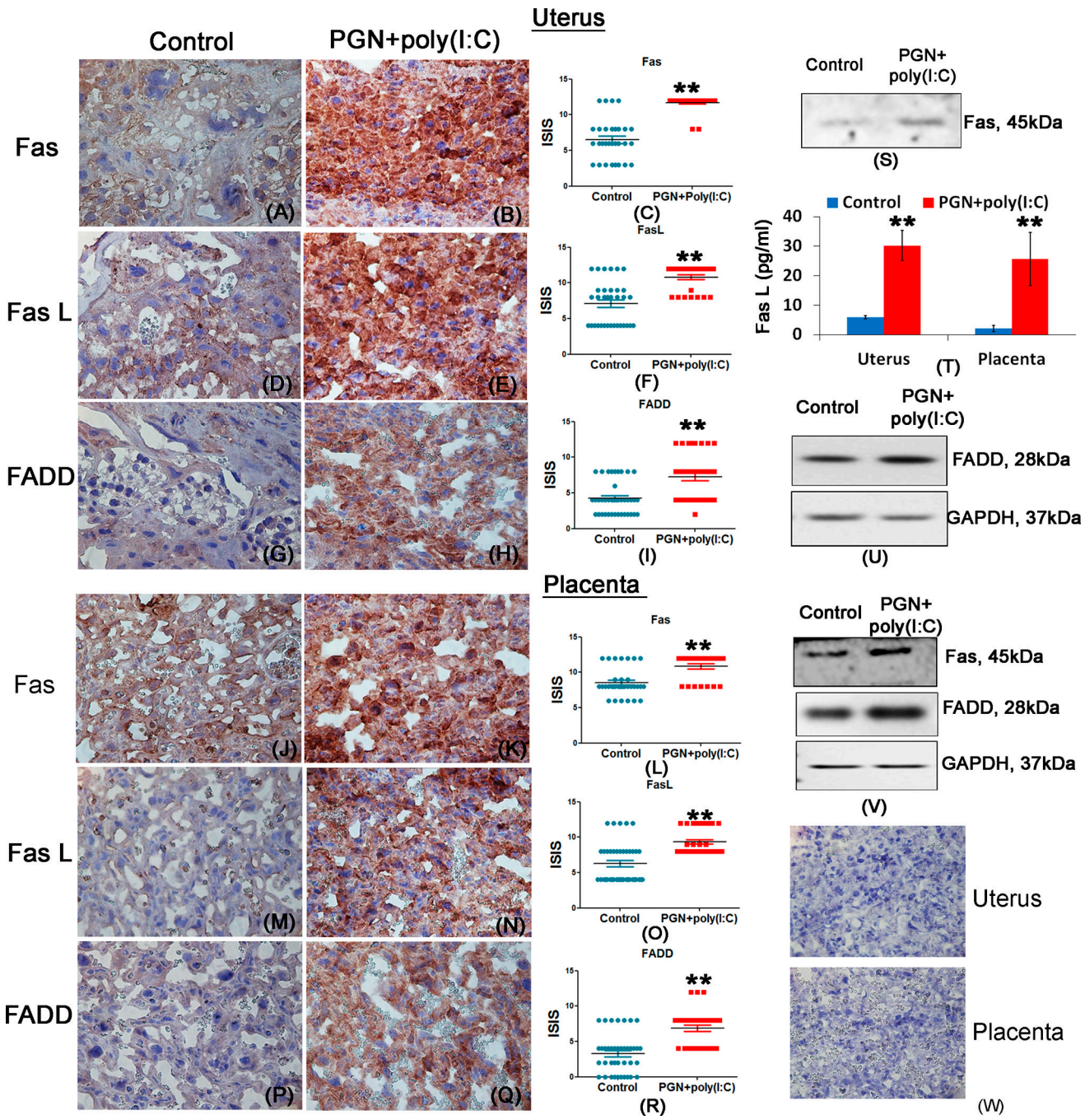

Figure 6. PGN+poly(I:C) induces apoptosis in the uterus and placenta via the extrinsic pathway

Immunolocalization of Fas, panel A–B and J–K; FasL, panel D–E and M–N; FADD, panel G–H and P–Q; in uterus and placenta recovered from the control and PGN+poly(I:C) treated groups. Panels C, F, I and L, O, R show the immunostaining index score (ISIS) in uterus and placentas recovered from control and PGN+poly(I:C) treated groups. Panel W shows isotype controls. Western blot analysis of Fas, panel S and V in uterus and placenta; Luminex assay of FasL, panel T in uterus and placenta; western blot analysis of FADD with GAPDH loading control, panel U and V in uterus and placenta recovered from the control and PGN +poly(I:C) treated groups. N=4–6 each group and six sections per animal were analyzed.

Error bars= ±SEM. **P≤0.01 Significant difference vs respective control. Original magnification: 400X.

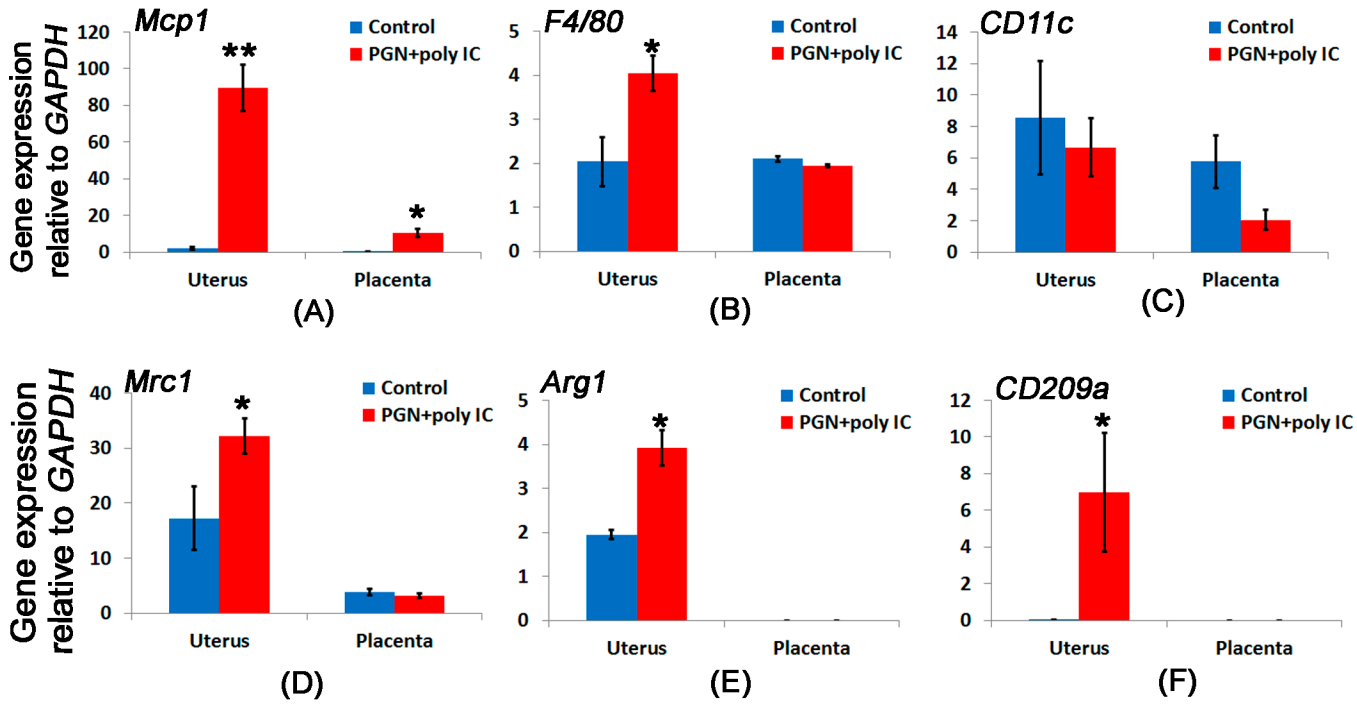

Figure 7. M2 like macrophage markers are increased in the PGN+poly(I:C) treated uterus

The bar diagram showing the mRNA expression of (A) *Mcp1* and, macrophage marker (B) *F4/80*, M1 macrophage marker (C) *CD11c*, M2 macrophage markers (D) *Mrc1*, (E) *Arg1*, and (F) *CD209a* in the uterus and placenta recovered from control and PGN+poly(I:C) treated groups. N=6 for control and n=11 for PGN+poly(I:C) treated group. Error bars= ±SEM. *P≤0.05, **P≤0.01 Significant difference vs respective control.

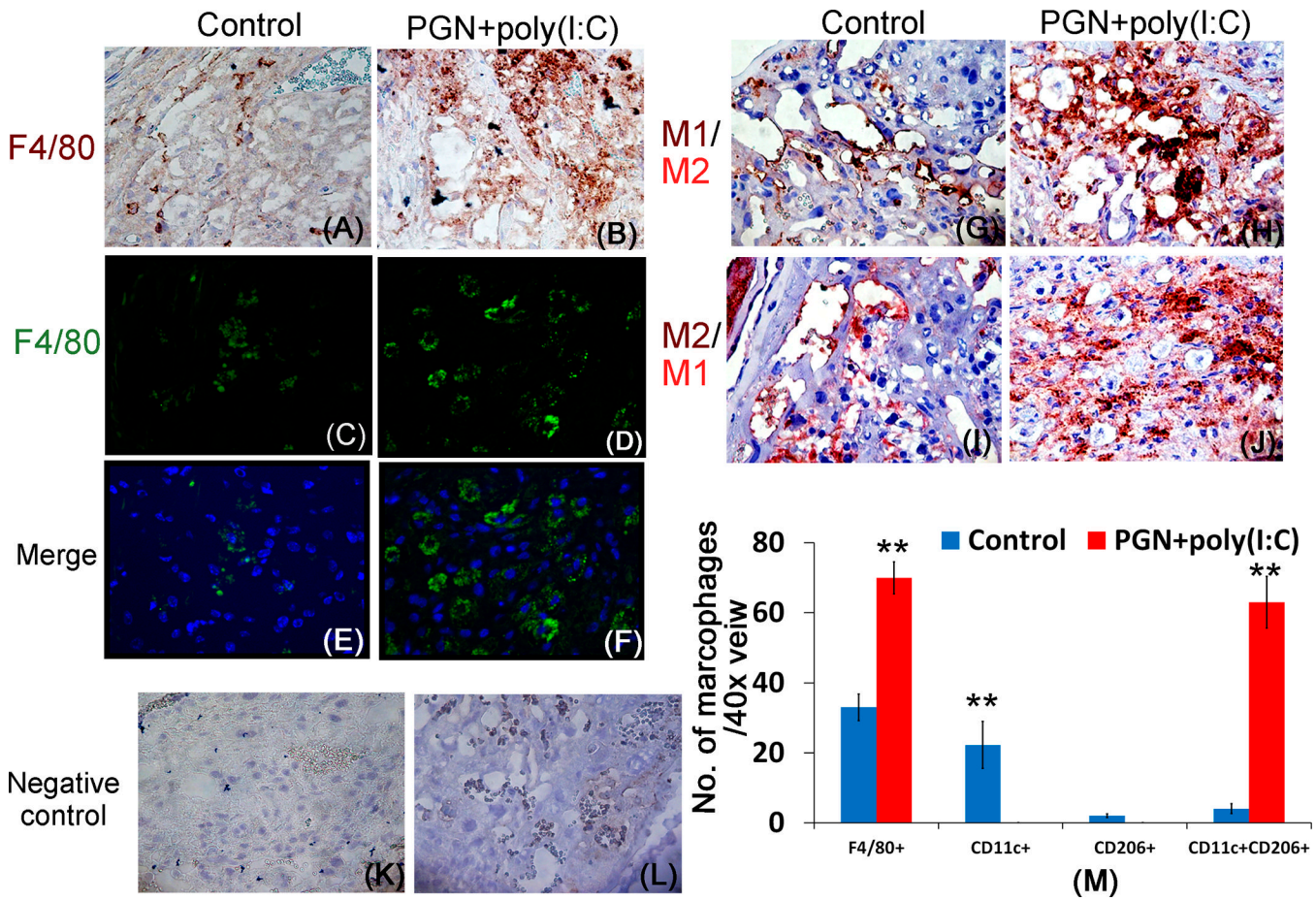

Figure 8. Macrophages are increased in the PGN+poly(I:C) treated uterus

Immunelocalization of F4/80 (brown) in control (A) and PGN+poly(I:C) treated (B) uterus. Original magnification: 400X. Immunofluorescence staining of F4/80 (FITC) in the control (C) and PGN+poly(I:C) treated uterus (D). Panel E and F are merged images (DAPI nuclear stain (blue), merged with FITC (stain F4/80) Original magnification: 200X. Immune-localization of CD11c (brown) and CD206 (red) in the control (G) and PGN+poly(I:C) treated (H) uterus; serial sections were stained in reverse order CD11c (red) and CD206 (brown) in control (I) and PGN+poly(I:C) treated (J) uterus showing that control uterine macrophages preferentially express CD11c while PGN+poly(I:C) treated uterine macrophages express both CD11c and CD206. Panel M shows the quantification of macrophages in the control and PGN+poly(I:C) treated uterus. Panels K and L show isotype controls. N=6 each group and six sections per animal were analyzed. Error bars= ±SEM. *P≤0.05, **P≤0.01 Significant difference vs respective control. Original magnification: 400X.

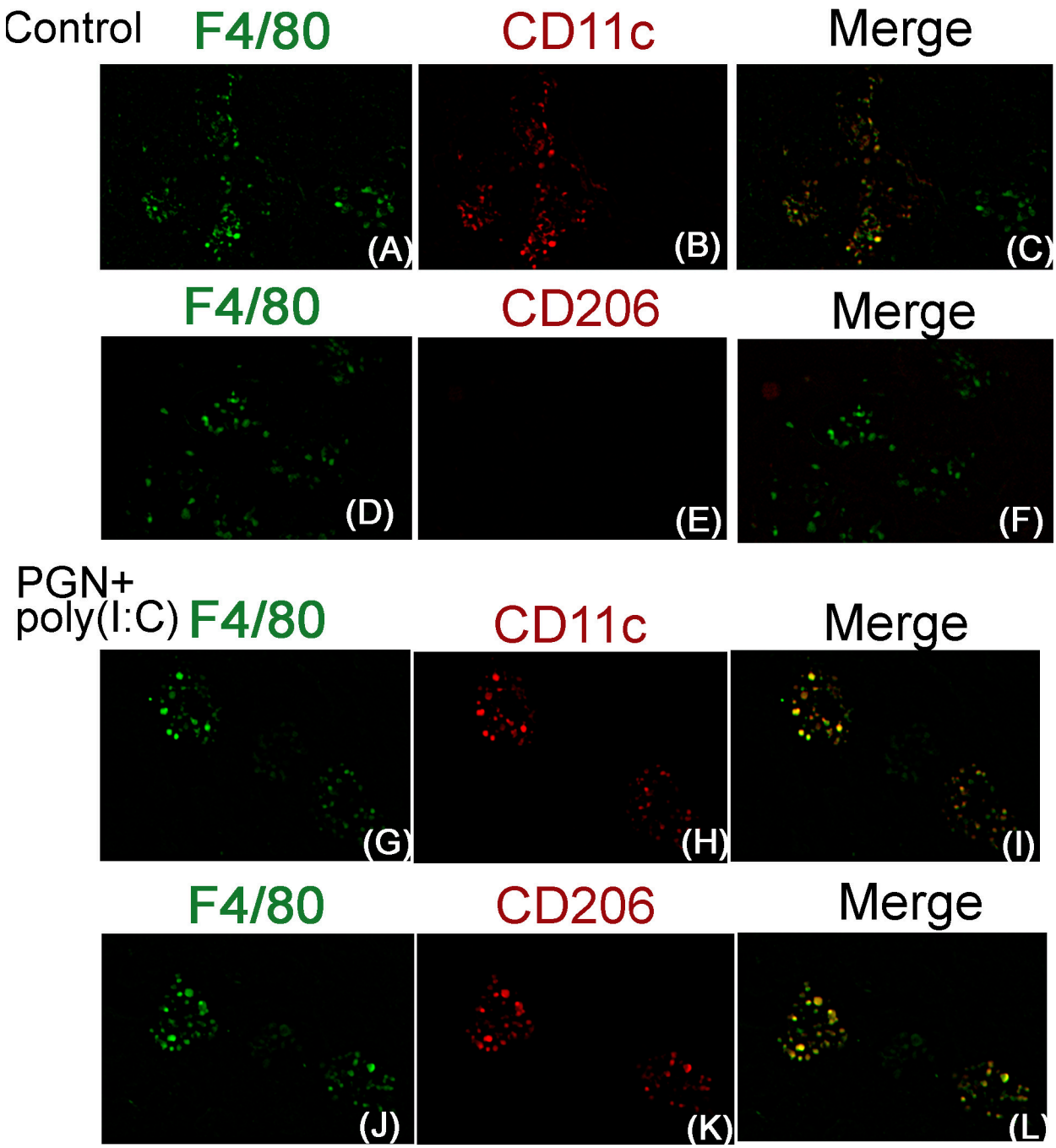

Figure 9. Uterine macrophage shift to double positive (CD11c+ and CD206+) during PGN +poly(I:C) induced preterm labor

Immunofluorescence of F4/80 (A), CD11c (B) and merged (F4/80 green, merged with CD11c red) (C) in control; and F4/80 (G), CD11c (H) and merged (I) in PGN+poly(I:C) treated uterus. Immunofluorescence of F4/80 (D), CD206 (E) and merged (F4/80 green, merged with CD206 red) (F) in control; and F4/80 (J), CD206 (K) and merged (L) in PGN +poly(I:C) treated uterus. N=6 each group and six sections per animal were analyzed. Original magnification: 400X.

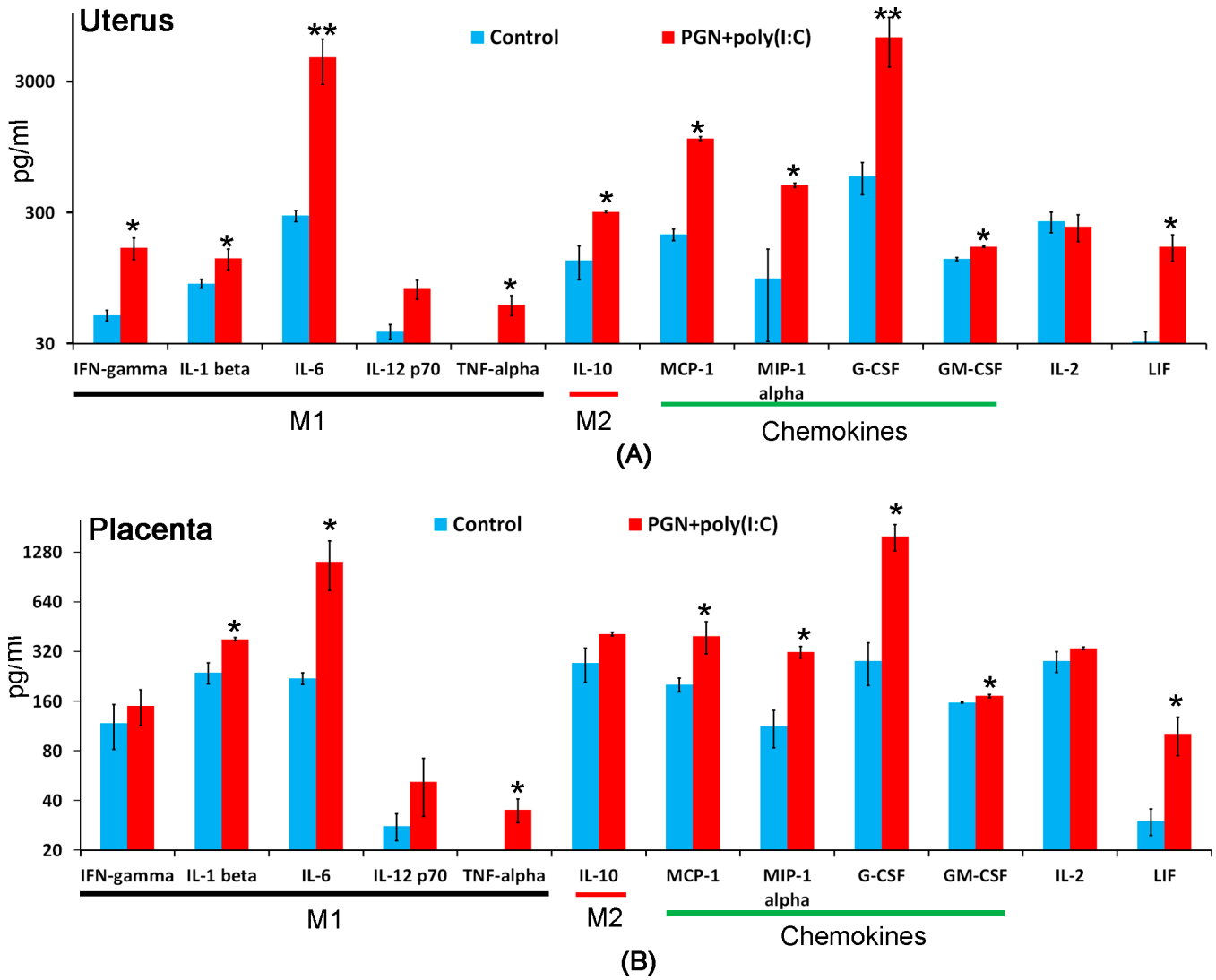

Figure 10. Cytokine and chemokine pattern during PGN+poly(I:C) induced preterm labor

M1 and M2 macrophage associated cytokines and other chemokines level were measured by luminex assay in uterus (A) and placenta (B) recovered from control and PGN+poly(I:C) treated animals. N=6 each group. Error bars= ±SEM. *P≤0.05, **P≤0.01 Significant difference vs respective control.

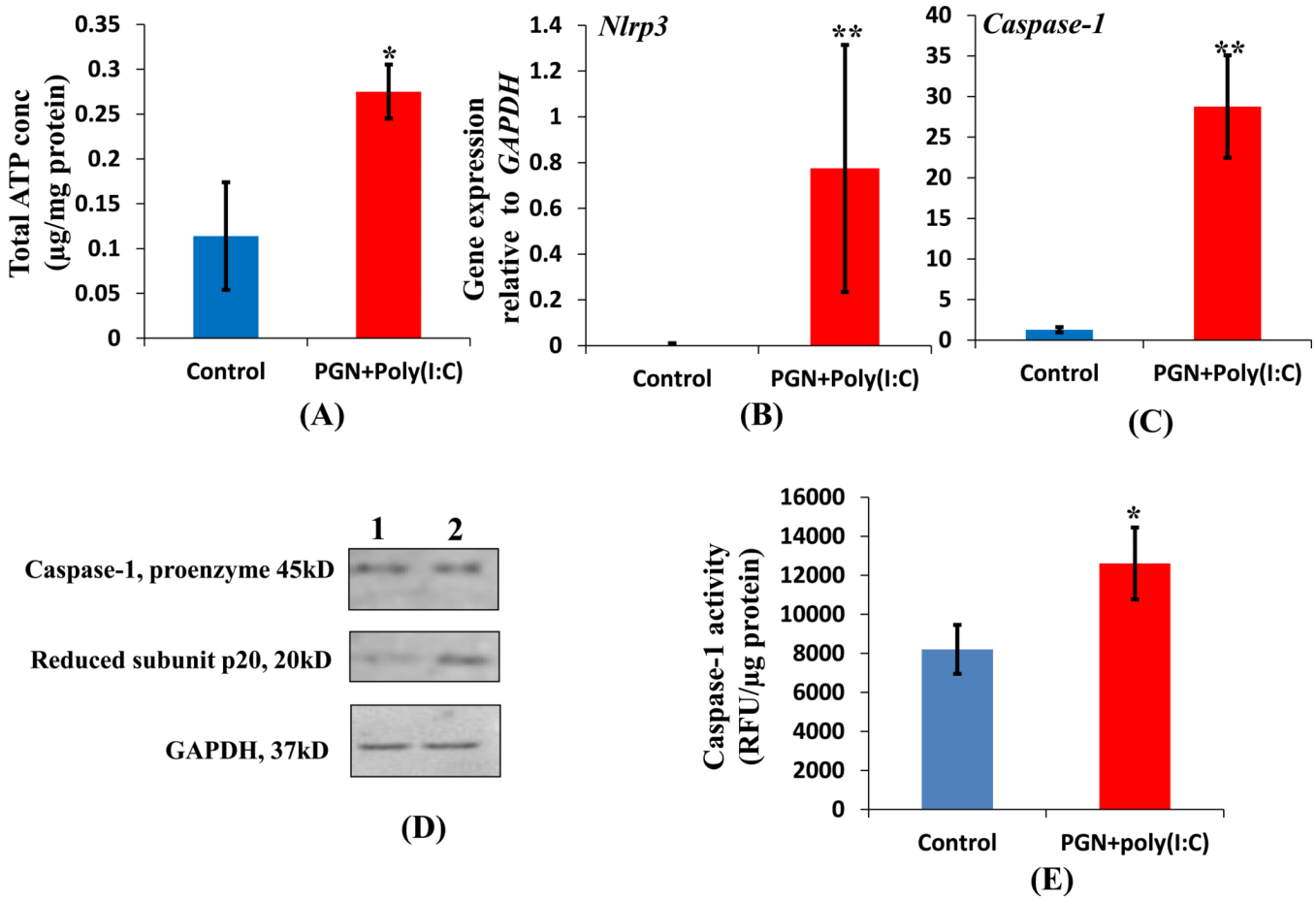

Figure 11. PGN+poly(I:C) induces inflammasome activation in uterus

Total ATP concentration (A); expression of *Nlrp3* (B); *Caspase-1* (C) in control and PGN +poly(I:C) treated uterus. N=6–11 each group. Panel D shows the level of activated caspase-1 in (lane 1) control and (lane 2) PGN+poly(I:C) treated uterus. Panel E show the caspase-1 activity. N=4–6 each group. Error bars=±SEM. *P≤0.05, **P≤0.01 Significant difference vs respective control.

Table 1

Decrease in gene expression and ISIS[a] of a2V in uterus and placenta correlated with preterm labor

Treatment	Tissues	Relative Gene expression of a2V	Protein level of a2V	Preterm delivery (%)
Control	*Uterus*	28.40±3.7	10.92±0.4	0/5 (0)
	Placenta	26.08±1.6	10.70±0.3	
	Fetal Membrane	12.15±2.1	-	
	Fetus	28.33±2.44	-	
PGN+poly (I:C)	*Uterus*	12.20±1.4*	6.62±0.5**	11/15 (73)
	Placenta	16.8±2.2*	7.7±0.4**	
	Fetal Membrane	5.89+1.45*	-	
	Fetus	28±2.63	-	

[a] Immunostaining index score (ISIS) = Stained area score (SAS) X Immunostaining intensity score (IIS)

** Significant difference vs. respective control; p≤0.01.